Title: Nanobiohybrids: New Model Systems for Membranes and Sensors

Principal Investigator: Emmanuel P. Giannelis

Address: Materials Science and Engineering, Bard Hall, Cornell University, Ithaca, NY 14853

Email: epg2@cornell.edu

Program Manager: Maj. Jennifer Gresham, PhD

Agreement Number: F49620-01-1-0512

June 2005

REPORT DOCUMENTATION PAGE

AFRL-SR-AR-TR-05-

0237

1. AGENCY USE ONLY *(Leave blank)*	2. REPORT DATE	3. REPORT TYPE AND DATES COVERED
	June 2005	FINAL

4. TITLE AND SUBTITLE
Nanobiohybrids: New Model Systems for Membranes and Sensors

5. FUNDING NUMBERS
F49620-01-1-0512

6. AUTHOR(S)
Giannelis, Emmanuel Pl

7. PERFORMING ORGANIZATION NAME(S) AND ADDRESS(ES)
Cornell University
Materials Science and Engineering
Bard Hall
Ithaca, NY 14853

8. PERFORMING ORGANIZATION REPORT NUMBER

9. SPONSORING/MONITORING AGENCY NAME(S) AND ADDRESS(ES)
AFOSR/NL
875 North Randolph Street
Suite 325, Rm 3112
Arlington, VA 22203

10. SPONSORING/MONITORING AGENCY REPORT NUMBER

11. SUPPLEMENTARY NOTES

12a. DISTRIBUTION AVAILABILITY STATEMENT
Approve for Public Release: Distribution Unlimited

12b. DISTRIBUTION CODE

13. ABSTRACT *(Maximum 200 words)*

The focus of this program is to correlate structure and function in biological membranes using nanohybrids as artificial models and to develop new sensors based on nanohybrids.

Nanohybrid artificial membranes exhibit characteristics similar to biological membranes and they can be used as sensors. The nanohybrid membranes are synthesized by intercalating amphiphile molecules into the galleries of a layered host producing an alternating amphiphile/inorganic multilayer. We have established how the nanohybrid membranes respond to changes in temperature, pH, pressure and electric field. For example, permeation through the nanohybrids can be modulated by changing the pH or by switching on and off the electric field across the membrane.

We have also shown that the nanohybrid membranes can be used as sensors for different analytes including sacchrine and quinine. Different responses have been observed even for molecules that have similar features for example, saccharin and its sodium salt suggesting that the nanohybrid might be useful in developing an electronic nose. The dynamic range of the current sensor for saccharin is 6μM to 500μM. Recent work has enabled us to optimize the response time (from several mintues to seconds) as well as better understand the sensing mechanism. We have found that the absorption of saccharin renders the membrane more hydrophilic. The more hydrophilic membrane allows for increased absorption of water molecules on both the surfaces and galleries of the membrane, which leads to changes in the electrostatic field and polarization of the membrane.

14. SUBJECT TERMS			15. NUMBER OF PAGES 15
			16. PRICE CODE
17. SECURITY CLASSIFICATION OF REPORT	18. SECURITY CLASSIFICATION OF THIS PAGE	19. SECURITY CLASSIFICATION OF ABSTRACT	20. LIMITATION OF ABSTRACT

June 22 05

Abstract

The focus of this program is to correlate structure and function in biological membranes using nanohybrids as artificial models and to develop new sensors based on nanohybrids.

Nanohybrid artificial membranes exhibit characteristics similar to biological membranes and they can be used as sensors. The nanohybrid membranes are synthesized by intercalating amphiphile molecules into the galleries of a layered host producing an alternating amphiphile/inorganic multilayer. We have established how the nanohybrid membranes respond to changes in temperature, pH, pressure and electric field. For example, permeation through the nanohybrids can be modulated by changing the pH or by switching on and off the electric field across the membrane.

We have also shown that the nanohybrid membranes can be used as sensors for different analytes including saccharin and quinine. Different responses have been observed even for molecules that have similar features for example, saccharin and its sodium salt suggesting that the nanohybrid might be useful in developing an electronic nose. The dynamic range of the current sensor for saccharin is 6μM to 500μM. Recent work has enabled us to optimize the response time (from several minutes to seconds) as well as better understand the sensing mechanism. We have found that adsorption of saccharin renders the membrane more hydrophilic. The more hydrophilic membrane allows for increased adsorption of water molecules on both the surfaces and galleries of the membrane, which leads to changes in the electrostatic field and polarization of the membrane.

Recently we have also focused on demonstrating more complex, biological functionality by introducing, for example, specific proteins and enzymes into the nanohybrids. When membrane proteins are inserted into supported lipid bilayers they are generally rendered non-functional because of the unfavorable interactions of the protein with the underlying substrate. We have developed a new method to immobilize membrane proteins that overcomes these problems. The method involves micellizing the protein into a mixture of ionic and non-ionic surfactants followed by intercalation into the galleries of the inorganic core. The immobilized proteins are in an environment similar to their natural habitat, which prevents them from being deactivated. The nanohybrid approach represents an excellent method to immobilize different biomolecules to prevent denaturing and develop active biohybrids for applications ranging from novel therapeutics to sensors.

Nanohybrids containing gramicidin show good selectivity (8x enhancement) towards sodium ions compared to control membranes (without the gramicidin). We have also synthesized glucose oxidase nanohybrids and demonstrated their sensing capability towards glucose. The sensor is fairly robust and reproducible.

Accomplishments –New Findings

Synthesis and Characterization of Bioinspired Artificial Membranes

Nanohybrids based on $2C_{18}N^{+}2C_1$ surfactant molecules and three different layered hosts - montmorillonite (MMT), fluoromica (FM) and fluorohectorite (FH) have been synthesized by ion-exchange. The bilayer forming amphiphiles replace native ions in the interlayer gallery of the inorganic host resulting in a multi-bilayer structure shown schematically in Figure 1.

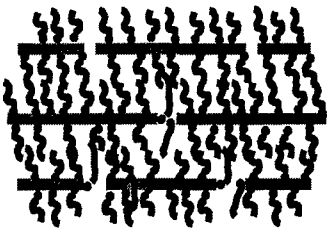

Figure 1. Schematic of an artificial membrane

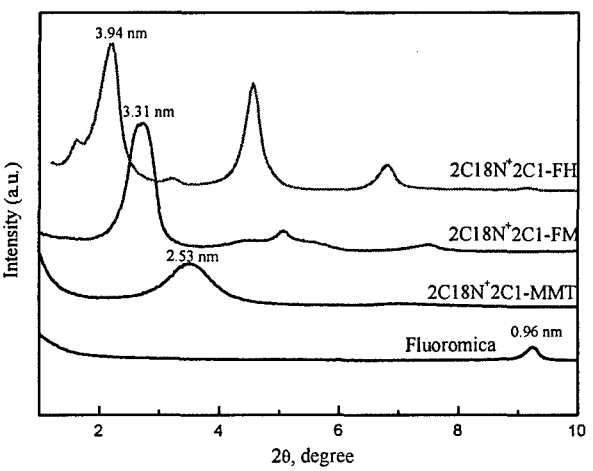

Figure 2. XRD patterns for the nanohybrids showing an increase in d-spacing upon ion-exchange with the surfactant molecules.

The d-spacing, and thus thickness of bilayer, (Figure 2) increase as the cation exchange capacity of the inorganic host increases (Table 1). As more and more surfactants are packed in the gallery, they are forced to adopt a more erect orientation resulting in a higher d-spacing.

Since the properties of membranes are evaluated at room as well as elevated temperatures we were interested in how temperature affects the d-spacing. The nanohybrids were equilibrated for 30 min at each temperature before measurement. Figure 3 shows that there is little change in bilayer thickness up to 100 °C.

Table 1. CEC and d-spacing for different nanohybrids

Host	CEC (meq/100g)	d-spacing (nm)
FM	120	3.3
FH	150	3.9
MMT	90	2.5

While there is very little change in bilayer thickness with temperature, the surfactant molecules undergo a transition upon heating. Figure 4 shows the DSC traces for the different nanohybrids. While the transition in the montmorillonite-based hybrid is rather broad, clear transitions are observed for the other two nanohybrids.

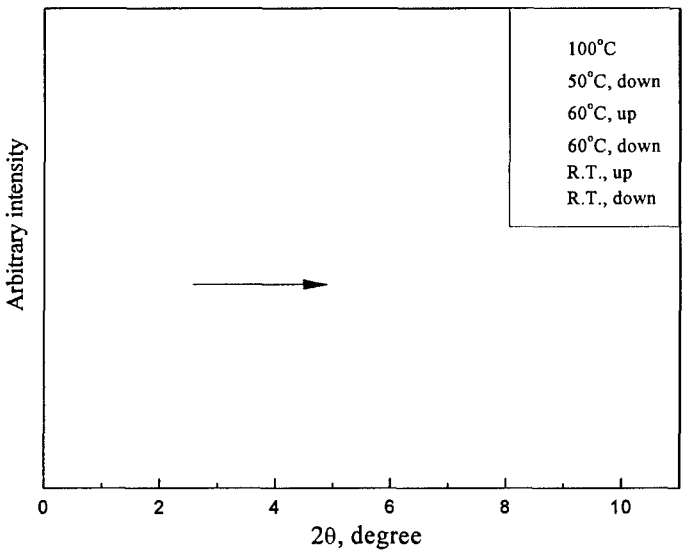

Figure 3. X-ray traces of nanohybrid membrane at different temperatures

The transitions observed in the DSC mirror a change in the conformation of the surfactant molecules (i.e. ratio of trans to gauche conformers) followed by FTIR (Figure 5). The frequency, peak height, and integrated intensity of the asymmetric and symmetric CH_2 stretching bands (near 2920 and 2850 cm^{-1}, respectively) are sensitive to gauche/trans conformer ratio of the hydrocarbon chains. At low temperatures the surfactant chains exhibit a solid-like behavior characterized by a peak at 2918 cm^{-1}. At the transition temperature the surfactants adopt a more disordered, liquid-like structure resulting from an increase in the gauche/trans conformations of the chains. This transition also corresponds nicely with the transport properties as permeation through the membrane

increases at the transition temperature (see below) due to an increase in the fluidity of the

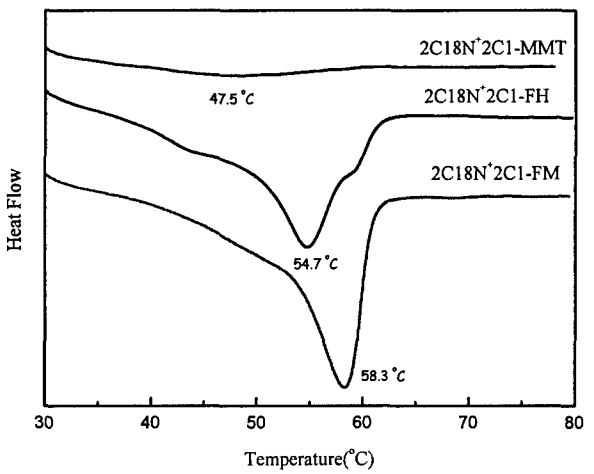

membrane.

Figure 4. DSC traces for different nanohybrid membranes.

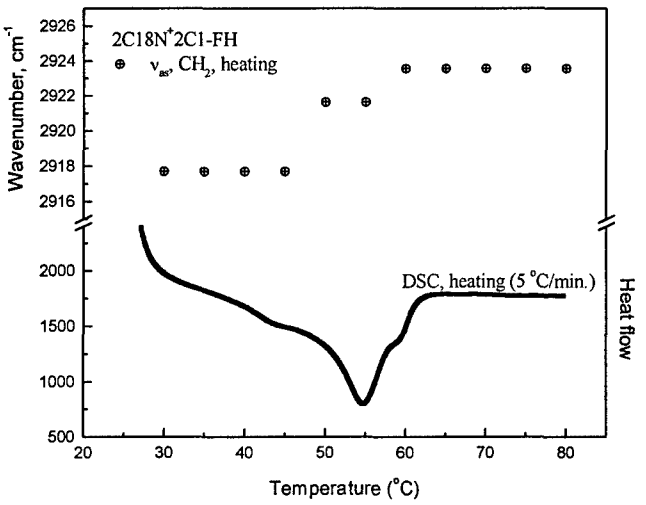

Figure 5. FTIR and DSC results showing both a transition near 55 °C.

Computer Simulations Studies

Molecular dynamics simulations were used to further characterize and understand the conformations and dynamics of the surfactant molecules at ambient and elevated temperatures. At ambient temperature (298K) the surfactant chains lie close to the host

surface forming a bilayer-like structure. As the temperature increases above the transition temperature as observed by DSC and FTIR the surfactant chains push away from the host surface and become more mobile evidenced by the appearance of multiple shoulders in the density profiles (Figures 6-8). **(and a faster decay of the end-to-end vector correlation function (Figure 9).**

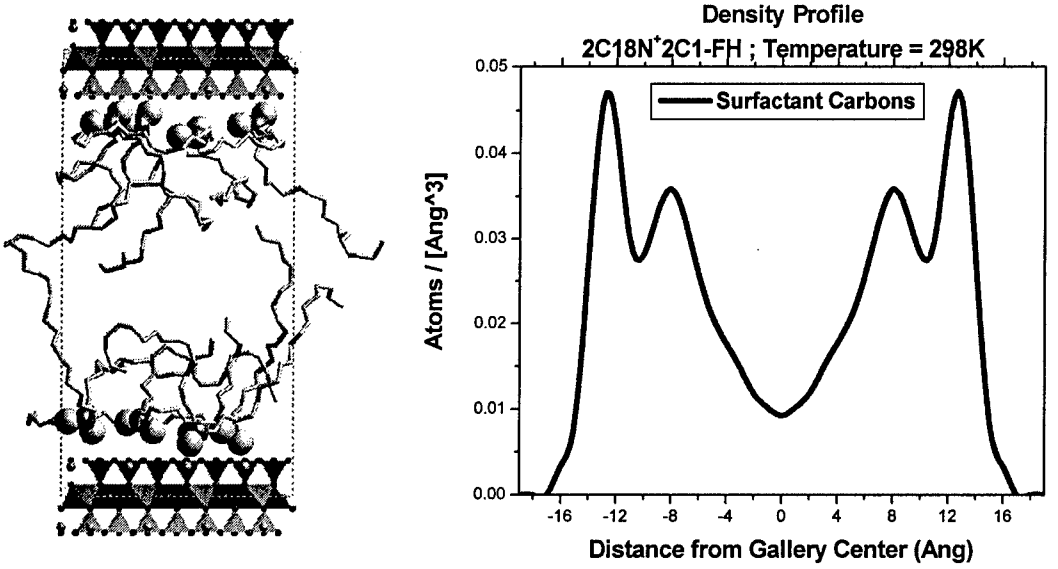

Figure 6. – MD Snapshot and Density profile of $2C18N^{+}2C1$-FH at 25°C

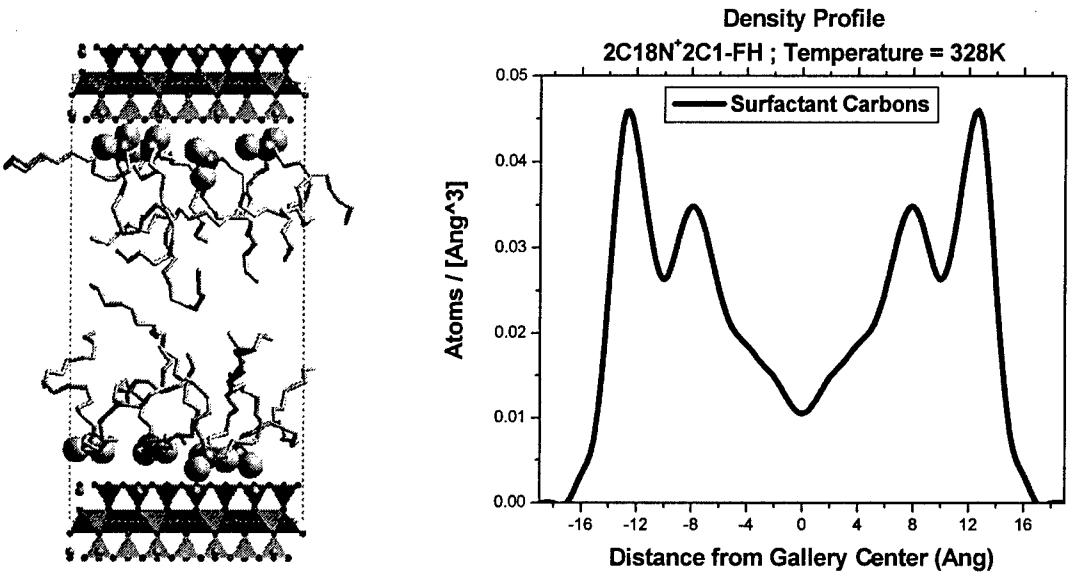

Figure 7. – MD Snapshot and Density profile of $2C18N^{+}2C1$-FH at 55°C

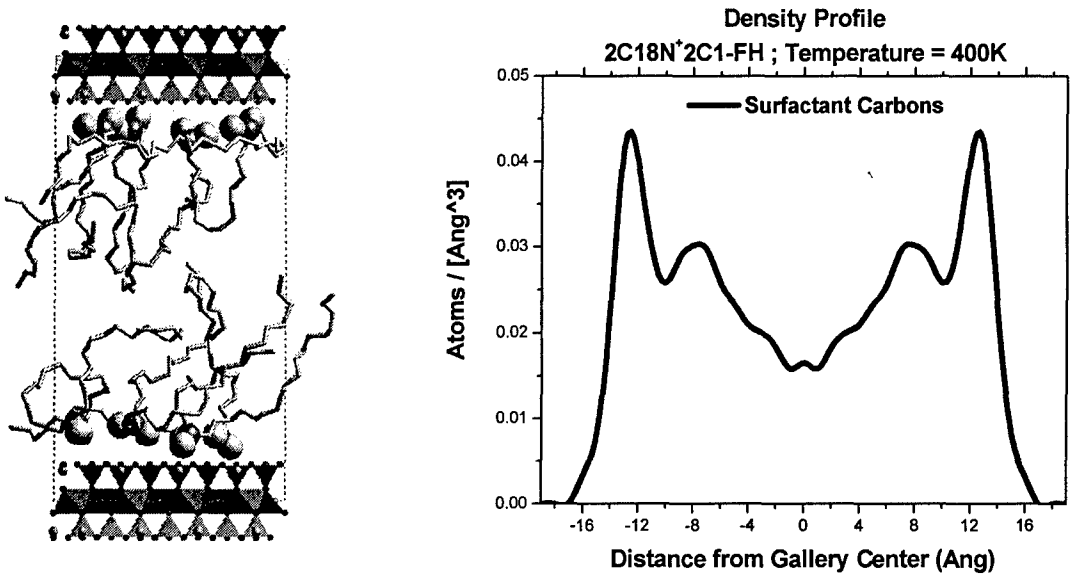

Figure 8. – MD Snapshot and Density profile of 2C18N$^+$2C1-FH at 127°C

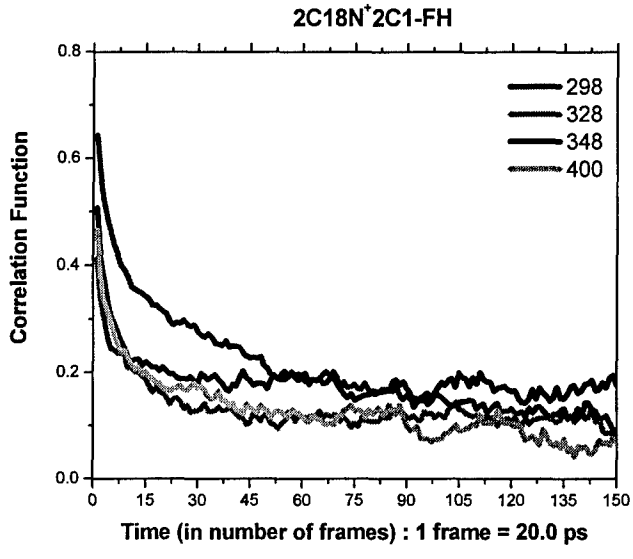

Figure 9. – End to end vector correlation function of surfactant chains in 2C18N$^+$2C1-FH

Transport Studies

For transport measurements membranes were cast from solution onto a 12-micron grid mesh. The experimental setup used is shown schematically in Figure 10. Using a dye solution and UV spectroscopy we were able to measure permeation and the flux through the membrane.

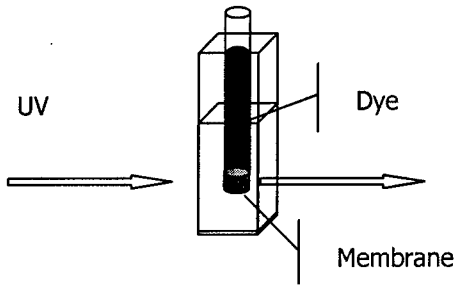

Figure 10. Experimental setup used for the permeation experiments

The thickness of the artificial membranes varied between 10 to 60 μm. The thickness depends on the concentration and the amount of casting solution used. Figures 11 and 12 show cross sections of nanohybrids based on fluorohectorite and fluoromica, respectively. While the resolution of the SEM is insufficient to distinguish individual layers, an overall morphology of parallel sheets can be easily seen.

Figure 11. Cross section SEM image of FH based nanohybrid.

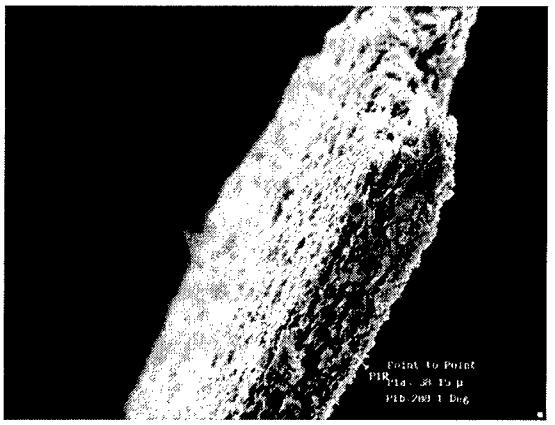

Figure 12. Cross section SEM image of FM based nanohybrid

For the transport experiments a solution of carminic acid (0.005M) was used. Both the effect of temperature and outside electric field (parallel and perpendicular to the membrane) on permeation has been evaluated.

Figure 13 shows the permeability of the nanohybrid membranes as a function of temperature. The permeability increases linearly with temperature up to the transition temperature observed by DSC and FTIR. At the transition temperature a sharp increase can be seen. We attribute the abrupt change in permeability to the change in membrane fluidity at the transition temperature as we discussed above.

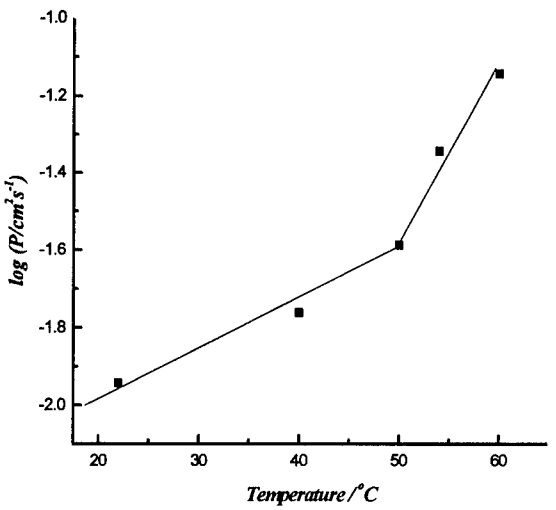

Figure 13. Permeability of FH-based nanohybrid at different temperatures

The values of permeability at ambient temperature are reproducible as shown in Table 2. The permeation rate scales inversely with thickness leading to similar permeabilities for membranes of different thickness.

Table 2. Room Temperature Permeability for Different Nanohybrid Membranes

Thickness (μm)	Temperature (°C)	Permeation Rate (s^{-1})
13	25	0.0008
12	27	0.0009
39	27	0.0003

Figure 14 demonstrates the effect of applied electric field on the permeation of the membrane. The experimental setup is shown schematically in Figure 15. When the field is parallel to the membrane there is no change in permeation by switching the field on or off. Doubling the field from 2.5 to 5 V does not have an effect either. In contrast, when the field is perpendicular to the membrane, switching the field on increases the flow through the membrane. The flow returns to its original value, when the field is switched off and the effect is reversible several times.

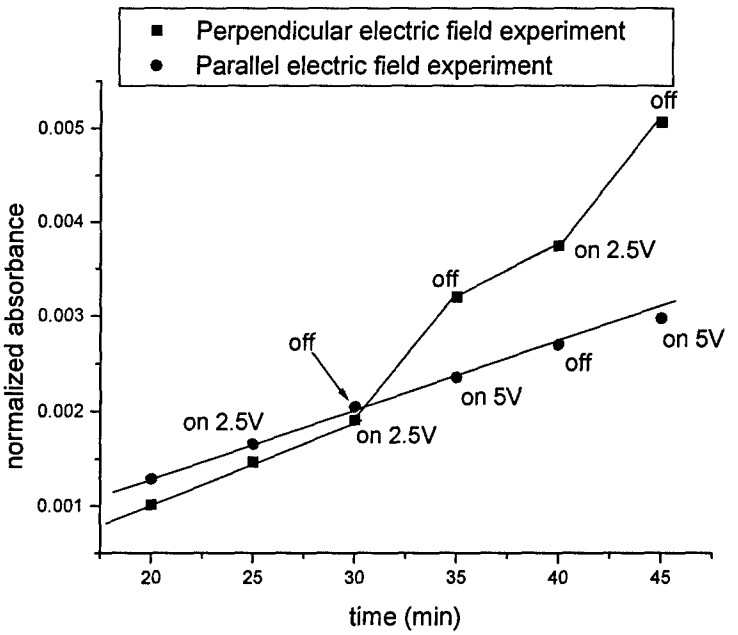

Figure 14. Effect of electrical field on the flow of nanohybrid membranes

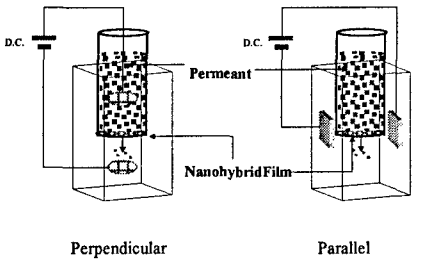

Figure 15. Experimental setup used for transport measurements in the presence of an electric field.

Nanohybrid Membranes as Sensors

While simple artificial membranes lack specific proteins they can still act as sensors. The working hypothesis is that the analyte interacts directly with the amphiphilic molecules and depolarizes the membrane.

To evaluate the sensing capability of our bioinspired membranes, films were formed on interdigitated electrodes (Figure 16) by solvent casting a suspension of the nanohybrid in toluene. After drying, membranes between 7-8 μm were obtained as measured by SEM. The membrane was immersed into a buffer containing beaker and known amounts of analyte were added. The electrical response was monitored by impedance spectroscopy. Measurements were made using a two-electrode array by applying a 10mV amplitude AC voltage and measuring the current and the phase angle through the electrodes.

Figure 17 shows the response of the nanohybrid membrane as rate of conductivity in the presence of saccharin. All conductance measurements were in the range of 200 to 400 μS falling into the linear log-log response of the electrodes. Using the rate of conductivity (i.e. the slope of conductivity over time) rather than conductivity per se we were able to decrease the response time of the sensor to a few seconds.

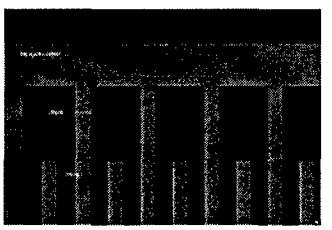

Figure 16. SEM picture of microfabricated interdigitated electrodes. Width of electrodes 20 microns.

The dynamic range of the current sensor is 6μM to 500μM. We expect further optimization of the size and the geometry of the electrodes to increase sensitivity. To evaluate the selectivity of the sensor, the response of our sensor to glucose and sucrose was investigated. No significant interference was found in the response of the sensor.

In an attempt to better understand the sensing mechanism and response of the nanohybrid membranes several experiments were designed to shed more light on how the analyte interacts with the membrane. Absorption of the analyte can cause a change in the hydrophilicity/hydrophobicity of the membrane. For example, if the membrane becomes more hydrophobic, more water molecules can be incorporated into the membrane. An increase in hydrophilicity, apart from increasing permeation of ions, can also change the "effective area" of the head group of the amphiphile and the orientation/association of water, which leads to changes in the electrostatic field at the surfaces of the membrane.

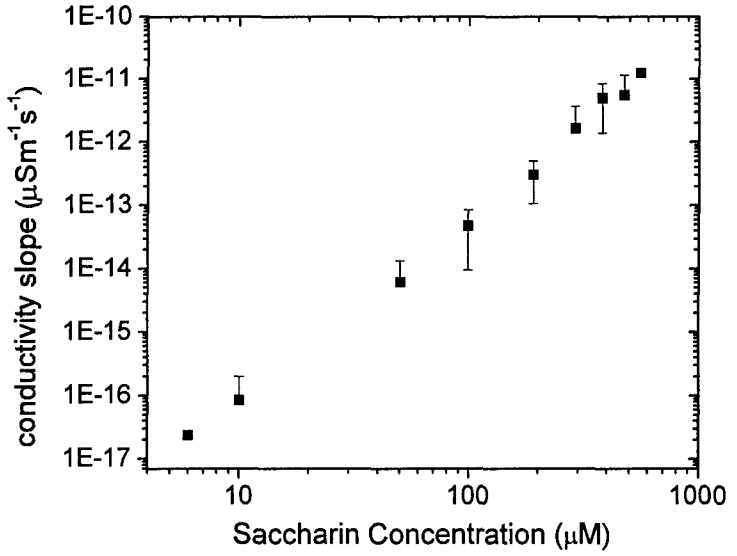

Figure 17. Response of nanohybrid sensor to saccharin

Contact angle measurements show a systematic decrease in contact angle with increasing saccharin content. The decrease in contact angle supports the suggestion that the membrane becomes more hydrophilic upon exposure to saccharin. X-ray diffraction profiles of the nanohybrid membrane show also a progressive increase in gallery height by 0.6 nm upon exposure to saccharin (Figure 18). The expansion is proportional to the concentration of the analyte solution for a given time and is due to the incorporation of water in the galleries of the nanohybrids.

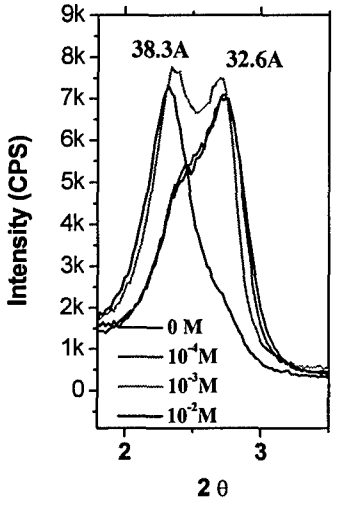

Figure 18. X-Ray diffraction patterns of nanohybrids exposed to progressively increasing concentrations of saccharin showing an increase in the gallery height from the original spacing attributed to intercalation of water molecules.

Gramicidin Nanohybrids

Integration of gramicidin was accomplished by ion exchanging gramicidin containing cationic micelles into the host nanoparticles shown schematically in Figure 19. The success of immobilization was investigated using X-ray diffraction, XRD, and FTIR. The nanohybrids exhibit the signature absorption peaks characteristic of gramicidin (amide peaks). In addition, an increase in the repeat unit of the organic/inorganic multilayer is consistent with the incorporation of gramicidin in the nanohybrid.

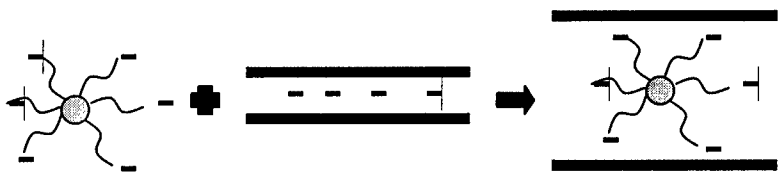

Figure 19. Schematic of the synthetic approach to introduce biomolecules like membrane proteins into the nanohybrids using micelles

Preliminary experiments show an increase in selectivity of the membrane towards sodium ions. Further experiments are in progress to evaluate the function of the nanohybrid membrane as an ion channel.

Glucose Nanohybrids-Sensors

Similar to gramicidin (i.e. by first encapsulating the biomolecule into a cationic micelle following by ion exchange) we have succeeded in incorporating Glucose oxidase in the nanohybrid membranes. XRD and FTIR suggest that the glucose oxidase has indeed been incorporated into the nanohybrids. Nanohybrid films were solution cast onto glass slides and their activity towards glucose was evaluated spectrophotometrically by monitoring by UV-Vis the color change accompanying exposure to glucose due to the production of H_2O_2 as shown below.

The slide with the enzyme containing nanohybrid was exposed to a solution of glucose for a given time (i.e. 3min). The hydrogen peroxide produced is assayed using o-tolidine as a substrate in the presence of horseradish peroxidase. The reaction from o-tolidine to p-tolidine turns the solution blue and the extent of reaction is measured spectrophotometrically.

The reactions can be seen below.

$$\text{Glucose} + 2H_2O + O_2 \xrightarrow{\text{Glucose Oxidase}} \text{Gluconic Acid} + 2H_2O_2$$

$$H_2O_2 + 2(\text{o-tolidine}) \xrightarrow{\text{Horseradish Peroxidase}} H_2O + 2(\text{p-tolidine})$$

Colorless **Blue**

The response of the glucose oxidase nanohybrid is shown in Figure 20. The nanohybrids were

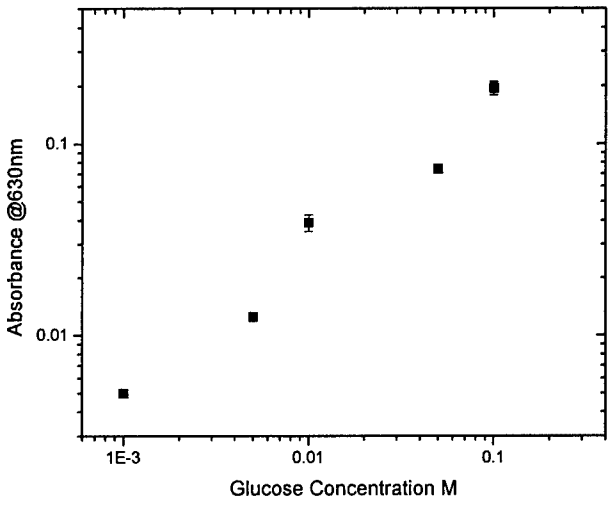

Figure 20. **Response of Glucose Oxidase Nanohybrid sensor**

active with a reproducible response up to 5 days. Further studies will focus on establishing a better understanding of the sensing mechanism as well as sensor optimization. Future work is also directed towards incorporation of other enzymes including catalase, urease and others.

Personnel Supported.

Nikolaos Chalkias (graduate student)

Evangelos Tsagarakis (visiting scientist)

Publications

130. K.M. Tyner, S. Schiffman and E.P. Giannelis, "Nanobiohybrids as Delivery Vehicles for Camptothecin", Journal of Controlled Release, 95, 501, **2004**.

131. K.M. Tyner, M.S. Roberson, K.A. Berghorn, L. Li, R.F. Gilmour Jr., and E.P. Giannelis, "Intercalation, Delivery, and Expression of the Gene Encoding Green Fluorescence Protein Utilizing Nanobiohybrids", Journal of Controlled Release, 100, 399, **2004**.

132. D. Shah, P. Maiti, E. Gunn, D.F. Schmidt, D.D. Jiang, C.A. Batt and E.P. Giannelis, "Dramatic Enhancements in Toughness of Polyvinylidene Fluoride Nanocomposites via Nanoclay-Directed Crystal Structure and Morphology", Advanced Materials, 16, 1173, **2004**.

133. D. Shah, P. Maiti, D.D. Jiang, C.A. Batt and E.P. Giannelis, "Effect of Nanoparticle Mobility on Toughness of Polymer Nanocomposites", Advanced Materials, 17, 525, **2005**.
134. A. B. Bourlinos, R. Herrera, N. Chalkias, D. D. Jiang, Q. Zhang, L. A. Archer, and E. P. Giannelis, "Solvent-Free Functionalized Nanoparticles with Liquid-like Behavior", Advanced Materials, 17, 234, **2005**.
135. A. B. Bourlinos, S.R. Chowdhury, D. D. Jiang, Y-U. An, Q. Zhang, L. A. Archer, and E. P. Giannelis, "Layered Organosilicate Nanoparticles with Liquid-like Behavior", Small, 1, 80, **2004**.
136. A. B. Bourlinos, K. Raman, R. Herrera, Q. Zhang, L. A. Archer, and E. P. Giannelis, "A Liquid Derivative of 12-Tungstophosphoric Acid with Unusually High Conductivity", Journal American Chemical Society, 126, 15358, **2004**
137. S.R. Scully, M.T. Lloyd, R. Herrera, E.P. Giannelis and G.G. Malliaras, "Dye Sensitized Solar Cells Employing a Highly Conductive and Mechanically Robust Nanocomposite Gel Electrolytes", Synthetic Metals, 144, 291, **2004**.
138. D. Shah, G. Fytas, D. Vlassopoulos, J. Di, D. Sogah, and E.P. Giannelis, "Structure and Dynamics of Polymer-Grafted Clay Suspensions", Langmuir, 21, 19, **2005**.
139. A.B. Bourlinos, S.R. Chowdhury, R. Herrera, D.D. Jiang, Q. Zhang, L.A. Archer, and E.P. Giannelis, "Functionalized Nanostructures with Liquid-like Behavior: Expanding the Gallery of Nanostructures", Advanced Functional Materials, in press.

Invited Talks to Conferences, Seminars

185.PPS-20, Akron, OH (June 2004)
186. ACMA Conference 2004, Tampa, FL (October 2004)
187. NERM, ACS, Rochester, NY (November 2004)
188. AAPS Annual Meeting, Baltimore, MD (November 2004)
189. Adhesion Society Annual Meeting, Mobile, AL (February 2005)
190. RSC, Workshop on New Materials for Drug Delivery, London, GB (February 2005)
191. Gordon Conference on Polymer Processing, Ventura, CA (March 2005)
192. ACS, "Polymers in Integrated Circuits", San Diego, CA (March 2005)
193. ACS, "Nanocomposites", San Diego, CA (March 2005)
194. 2005 Symposium on Polymer Nanocomposites, Columbia, SC (April 2005)
195. University of Rochester, Rochester, NY (April 2005)
196. Norfolk State University, Norfolk, VA (April 2005)

Invited Seminars to Industry

129. Pactiv, Canandaigua, NY (June 2004)
130. UOP, Des Plaines, IL (June 2004)
131. Eastman Kodak, Rochester, NY (September 2004)
132. Eastman Kodak, Rochester, NY (October 2004)

133. Bristol-Myers Squibb, New Brunswick, NJ (October 2004)
134. Intel, Chandler, AZ (October 2004)
135. Procter and Gamble, Cincinnati, OH (November 2004)
136. Bayer, Leverkusen Germany (January 2005)
137. Bayer, Uerdingen Germany (February 2005)
138. Essilor, St. Petersburg, FL (February 2005)
139. Sherwin Williams, Cleveland, OH (March 2005)

Interactions/Transitions

We are collaborating with Bristol-Myers-Squibb to evaluate the use of nanohybrids as a means to increase the solubility and bioavailability of water insoluble drugs.

New discoveries, inventions, or patent disclosures.

1. A.B. Bourlinos and E.P. Giannelis, "Functionalized Nanostructures with Liquid-like Bahavior".

Honors/Awards

EPG, Member of Editorial Board, *Polymer*